

N 9 3 - 1 7 4 0 2

## A ROSAT HIGH RESOLUTION X-RAY IMAGE OF NGC 1068

J. Halpern, Columbia University, New York, NY 10027

## ABSTRACT

The soft X-ray properties of the Seyfert 2 galaxy NGC 1068 are a crucial test of the "hidden Seyfert 1" model. It is important to determine whether the soft X-rays come from the nucleus, or from a number of other possible regions in the circumnuclear starburst disk. We present preliminary results of a ROSAT HRI observation of NGC 1068 obtained during the verification phase. The fraction of X-rays that can be attributed to the nucleus is about 70%, so the "soft X-ray problem" remains. There is also significant diffuse X-ray flux on arcminute scales, which may be related to the "diffuse ionized medium" seen in optical emission lines, and the highly ionized Fe K $\alpha$  emission seen by BBXRT.

## INTRODUCTION

In the hidden Seyfert 1 model of NGC 1068 (Antonucci and Miller 1985), the ionizing flux is seen only indirectly via electron scattering from a warm, ionized medium above the axis of an obscuring molecular torus. The results of spectropolarimetry of the Balmer lines require that the electron temperature in the scattering region is  $\leq 3 \times 10^5$  K (Miller *et al.* 1991, hereafter MGM). It is difficult, but not impossible, for soft X-rays to emerge unabsorbed through a gas at this low temperature (Monier and Halpern 1987). Careful fine tuning of the photoionization model is required to avoid imprinting absorption or emission features on the soft X-ray spectrum (MGM). This problem would be avoided entirely if the soft X-rays are *not* coming from the nucleus, a reasonable expectation since NGC 1068 is also a bright starburst galaxy.

## RESULTS

A 20,000 s observation of NGC 1068 was obtained with the ROSAT HRI between July 24 and 26, 1990. The observed X-ray luminosity of NGC 1068 in the 0.1 - 2.4 keV band is  $\sim 9 \times 10^{41}$  ergs s $^{-1}$  (for a distance of 22 Mpc), consistent with previous measurements. The central region of the HRI image is shown in Figure 1, and an X-ray contour map of the galaxy is shown in Figure 2. There is a "nuclear" source, which is characterized by FWHM = 5".5 in the east-west direction, and 7" in the north-south direction. This is close to the theoretical FWHM of 5" which is expected to result when the effects of mirror and detector resolution, and aspect solution are combined. There is not yet enough calibration data available to test whether the marginal extent in the north-south direction is real. The fraction of X-rays from NGC 1068 that can be attributed to the "nucleus" is about 70%, as indicated by the X-ray flux within a radius of 9", which is 3 sigmas of the radial Gaussian corresponding to the observed FWHM.

There is also significant diffuse X-ray flux on an arcminute scale. It covers much of the galaxy, and is elongated at position angle  $\sim 35^\circ$ , which is similar to that of the nuclear radio structure (Wilson and Ulvestad 1983). The surface brightness is greatest in the northeast, which is the direction of the one-sided ionization cone (Pogge 1988) and the region of strong, high-excitation [Ne V]

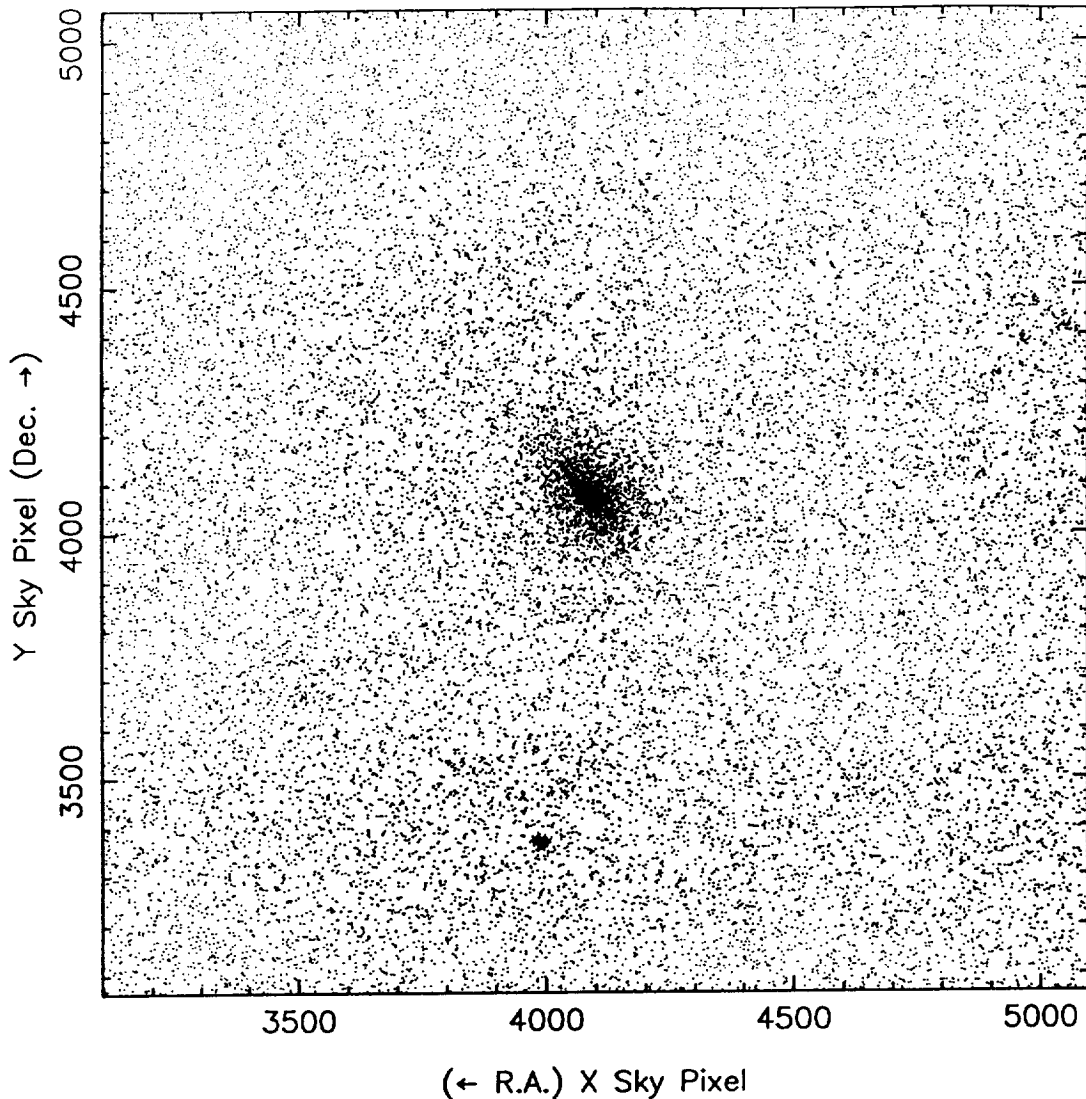


FIG. 1. - The ROSAT HRI image of NGC 1068, showing the central  $16'.7 \times 16'.7$  of the field. Each dot represents one photon. Approximately 11,700 photons are detected in a region of radius  $2'$  centered on NGC 1068, of which  $\sim 70\%$  can be attributed to the nucleus. A stellar source is also detected  $5'.8$  south of the galaxy.

$\lambda 3426$  emission (Evans and Dopita 1986; Bergeron *et al.* 1989). In the northeast direction, the diffuse X-ray emission extends as far as the large-scale 20 cm radio emission of the disk (Wilson and Ulvestad 1982). The diffuse luminosity within a  $1'$  radius (6 kpc) is  $\sim 4 \times 10^{41}$  ergs  $s^{-1}$  when corrected for Galactic  $N_H = 3 \times 10^{20}$   $cm^{-2}$ , which is comparable to that of other bright starburst galaxies (Ward 1988). Similar luminosities of extended X-ray emission were detected in *Einstein* HRI images of several Seyfert 1 galaxies (Elvis *et al.* 1990). In NGC 1068, about 20% of the total X-ray flux comes from a region which is larger than the  $30''$  diameter starburst disk.

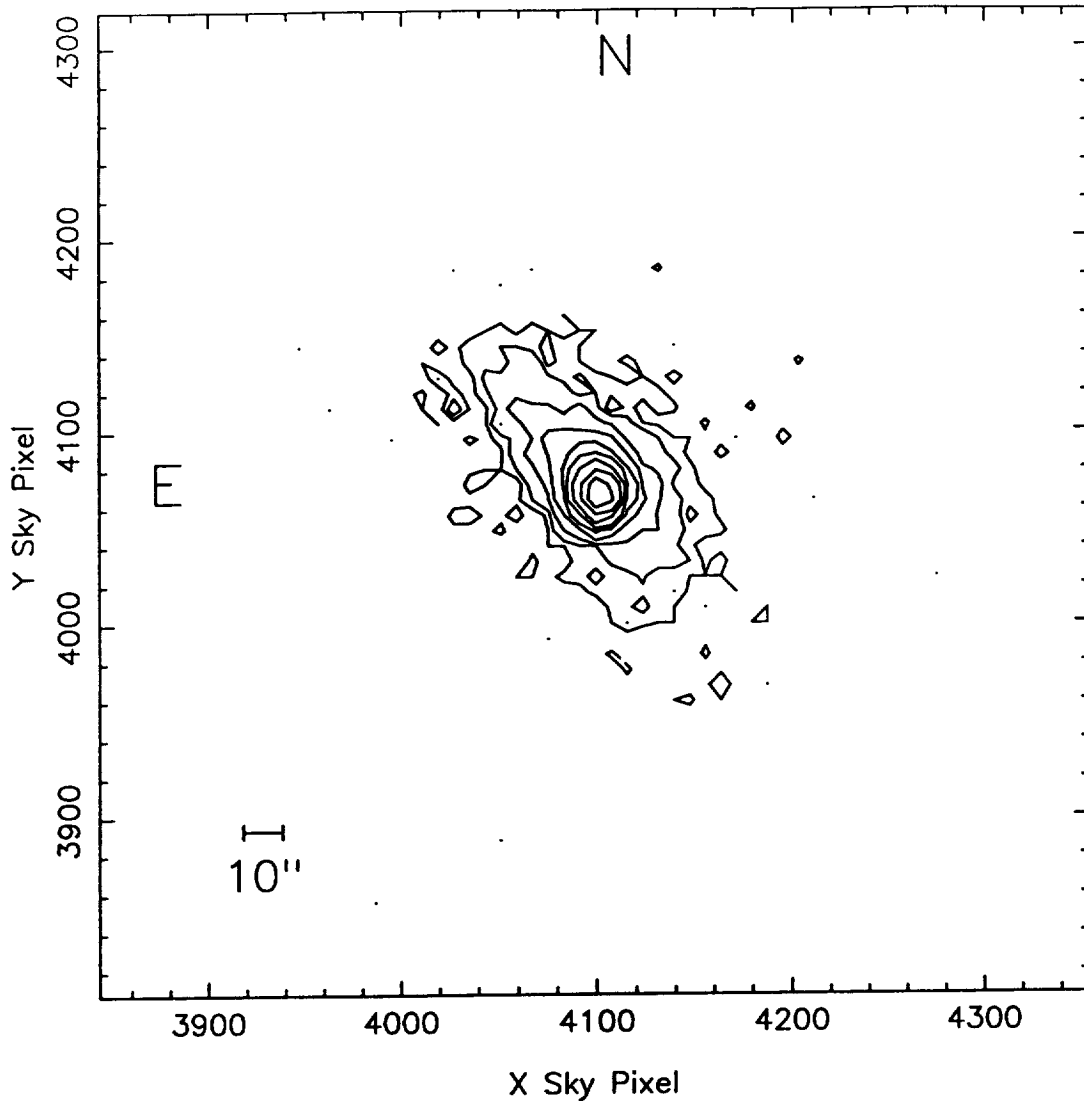


FIG. 2. - Contour map of the X-ray image of NGC 1068. The field is  $4' \times 4'$ . The image has been binned into  $4'' \times 4''$  pixels. The lowest contour level corresponds to an intensity of 4 counts per pixel, or a flux of  $\sim 1.5 \times 10^{-14}$  ergs  $\text{cm}^{-2} \text{s}^{-1}$ . The contour levels are separated by factors of 2 in intensity.

### INTERPRETATION

The detection of a nuclear soft X-ray source, in combination with the lack of oxygen features in the BBXRT spectrum (Marshall 1992), presents a significant challenge to the electron scattering model. The emergent X-ray spectrum should have either a K-edge of  $\text{O}^{+7}$  at 870 eV (Monier and Halpern 1987), or a  $\text{Ly}\alpha$  recombination line at 654 eV, neither of which are seen (Marshall 1992). One can wriggle out of the problem by noting that the “nuclear” HRI source, with its instrumental resolution of 500 pc, may still be outside the scattering region, for which the theory of MGM favors only a lower limit of 30 pc.

The diffuse X-ray flux is similar in extent to the "diffuse ionized medium" seen in the [N II] and H $\alpha$  imaging Fabry-Perot data of Bland-Hawthorn *et al.* (1991). Unlike H II regions, the ratio [N II]  $\lambda$ 6584/H $\alpha$  is greater than 1. The large velocity widths of the lines in comparison with the adjacent H II regions, led these authors to predict that the scale height of the emitting filaments might be high,  $\sim 400$  pc, and that they might be confined by, or condense out of, a hot phase which would be seen by ROSAT. The HRI image is substantially in agreement with this prediction. Since some of the X-ray flux comes from a region which is larger than the 30" diameter starburst disk, it is likely to originate in a diffuse hot medium, rather than numerous discrete supernova remnants or binary X-ray sources. To explain the diffuse X-ray emission as bremsstrahlung at  $T \sim 10^7$  K, we require emission measure  $n_e^2 V \sim 7 \times 10^{64}$  cm $^{-3}$ , or electron density  $n_e \sim 0.15$  over the inner 6 kpc radius and 400 pc scale height. This medium would also be responsible for the He and H-like iron lines seen in the BBXRT spectrum, which requires  $n_e^2 V \sim 1.5 \times 10^{64}$  cm $^{-3}$  at  $T \sim 10^7$  K (Marshall 1992). It could also exist in pressure balance with optical filaments of density  $\sim 100$  cm $^{-3}$  and filling factor  $\sim 10^{-6}$ .

The cooling rate of the optical filaments is estimated to be  $\sim 4 \times 10^{42}$  ergs s $^{-1}$  (Sokolowski *et al.* 1991), while the diffuse X-ray luminosity is ten times smaller. Photoionization by the active nucleus is an ample source of energy for both the optical filaments and the X-ray emitting gas, although the ionization parameter may not be high enough to heat the low-density medium to  $10^7$  K. In the context of the obscuring torus/electron scattering model, the *intrinsic* ionizing luminosity  $L$  of the nucleus is related to the *observed* luminosity  $L_o$  via  $L = (1/\tau_{es})(4\pi/\Omega)L_o$ , where  $\Omega$  is the unobscured solid angle. Estimates of  $L$  range between  $7 \times 10^{43}$  and  $1 \times 10^{45}$  ergs s $^{-1}$  (Monier and Halpern 1987; Sokolowski *et al.* 1991), or even higher if there is intrinsic beaming (MGM). So the diffuse optical filaments need only absorb  $\sim 1\%$  of the nuclear luminosity to power the emission lines. However, the ionization parameter ( $\xi = L_x/nr^2$ ) must be  $\sim 1000$  in the X-ray emitting medium for He and H-like iron to predominate. This can only occur if the nuclear luminosity is  $\geq 10^{45}$  ergs s $^{-1}$ , as estimated by MGM. Alternatively, shock heating by supernova remnants or energetic stellar winds may contribute to the energetics of the diffuse X-ray emitting gas.

## REFERENCES

- Antonucci, R. R., and Miller, J. S. 1985, *Ap. J.*, **297**, 621.  
 Bergeron, J., Petitjean, P., and Durret, F. 1989, *Astr. Ap.*, **213**, 61.  
 Bland-Hawthorn, J., Sokolowski, J., and Cecil, G. 1991, *Ap. J.*, **375**, 78.  
 Elvis, M., Fassnacht, C., Wilson, A. S., and Briel, U. 1990, *Ap. J.*, **361** 459.  
 Evans, I. N., and Dopita, M. A. 1986, *Ap. J. (Letters)*, **310**, L15.  
 Marshall, F. E. 1992, this volume.  
 Miller, J. S., Goodrich, R. W., and Mathews, W. G. 1991, *Ap. J.*, **378**, 47 (MGM).  
 Monier, R., and Halpern, J. P. 1989, *Ap. J. (Letters)*, **315**, L17.  
 Pogge, R. 1988, *Ap. J.*, **328**, 519.  
 Sokolowski, J. K., Bland-Hawthorn, J., and Cecil, G. 1991, *Ap. J.*, **375**, 583.  
 Ward, M. J. 1988, *M.N.R.A.S.*, **231**, 1P.  
 Wilson, A. S., and Ulvestad, J. S. 1982, *Ap. J.*, **263**, 576.  
 Wilson, A. S., and Ulvestad, J. S. 1983, *Ap. J.*, **275**, 8.

## Discovery of soft X-ray pulsations from the $\gamma$ -ray source Geminga

J. P. Halpern\* & S. S. Holt†

\* Columbia Astrophysics Laboratory, Columbia University,  
538 West 120th Street, New York, New York 10027, USA

† Director of Space Sciences, Code 600, NASA Goddard Space  
Flight Center, Greenbelt, Maryland 20771, USA

THE nature of the  $\gamma$ -ray source 'Geminga' (2CG195+04) is a problem of considerable importance in high-energy astrophysics. First discovered in 1972 by the SAS-2 satellite<sup>1</sup>, Geminga emits virtually all its power at energies above 50 MeV, and at energies above 100 MeV is the second brightest source in the  $\gamma$ -ray sky survey made by the Cos-B satellite<sup>2</sup>. It eluded identification at all other wavelengths until the Einstein Observatory found an unusual soft X-ray source, 1E0630+178, in its error box<sup>3</sup>. This source also has a claimed twenty-fifth magnitude optical counterpart<sup>4-6</sup>. This distinctive set of properties is reminiscent of the Vela pulsar, except for the absence of radio emission<sup>7</sup> or a synchrotron nebula<sup>8</sup>. We have made a more sensitive soft X-ray observation of the Geminga field using Rosat, and have detected coherent pulsations from 1E0630+178 at a period of 0.237 s. This result confirms suggestions<sup>3-6,8,9</sup> that Geminga is, like Vela, a  $\gamma$ -ray pulsar. We speculate that Geminga is somewhat the older of the two. With this discovery we consider the mystery of Geminga largely solved.

For Geminga, the soft X-ray band is the most promising one for a pulsar search because the count rate is high and the background is negligible. The Geminga field was observed with the Position Sensitive Proportional Counter (PSPC) aboard Rosat<sup>10</sup> during 1991 March 14-17. A total of 14,390 s of exposure were obtained during 10 satellite orbits as listed in Table 1. The mean count rate of 1E0630+178 was  $0.53 \text{ s}^{-1}$  in the 0.07-2.4-keV band. A total of 7,630 counts were detected within a circle of radius 1.5' about the source centroid, of which only ~1% are background. After transforming the photon arrival times to the barycentre of the Solar System using the accurate (~3") Einstein High Resolution Imager position, the search for periodicity was

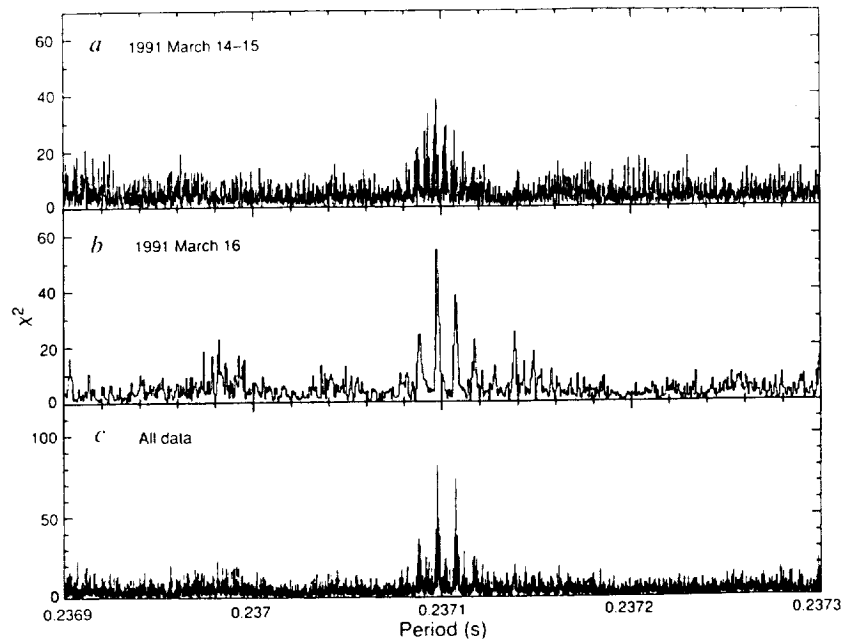
TABLE 1 Rosat observations of Geminga

Date (UT)	Start time (s)	Duration (s)	Counts
1991 March 14	76,564	1,193	612
1991 March 15	1,191	1,437	749
1991 March 15	29,362	1,360	703
1991 March 15	64,656	1,567	866
1991 March 15	76,468	1,272	641
1991 March 16	64,514	1,690	887
1991 March 16	69,999	1,959	1,038
1991 March 16	76,448	1,272	724
1991 March 16	81,745	1,509	786
1991 March 17	46,703	1,131	624

begun by performing a fast Fourier transform (FFT) on the section of data consisting of four consecutive orbits on March 16. The FFT covered 262,144 independent trial periods down to a minimum period of 0.072 s. The only significant peak in the power spectrum occurred at a period of 0.237097 s, for which the power is 17.5 times the mean. The probability that a peak of this strength or greater will occur by chance somewhere in the power spectrum is 0.007. The same section of data was then folded about a range of trial periods. The  $\chi^2$  values of the resulting five-bin folded light curves were calculated with respect to a constant mean. The candidate period appeared with  $\chi^2 = 39.5$  for 4 degrees of freedom. The probability that  $\chi^2$  greater than or equal to this value will occur by chance in a single trial is  $6 \times 10^{-8}$ . When multiplied by the number of trial periods, the chance probability is 0.016. The highest  $\chi^2$  in the periodogram of the folded data is 54.7 (Fig. 1b). The single-trial chance probability is less than  $10^{-10}$ , but the effective number of periods searched in the epoch folding is about a factor of 5 higher than in the FFT. We conclude that the probability that the period is spurious is  $\leq 1 \times 10^{-4}$ .

The reality of the signal at 0.237 s is further supported by its presence in the remaining half of the data which was not included in the original FFT. Figure 1a shows the periodogram for the five orbits of data obtained on March 14-15. The period is clearly indicated in this independent set of data, although the less-than-optimal sampling introduces many more aliases at the 96-min satellite orbital period and its multiples. Figure 1c is the result of the coherent folding of data from all 10 orbits. The

FIG. 1 Periodograms of the five-bin folded light curves. The multiple peaks are aliases of the 96-min satellite orbital period. The best-fit period is  $0.2370974 \text{ s} \pm 0.1 \text{ } \mu\text{s}$ .



highest peaks in all three panels are at the same period to within the errors. The symmetry of the peak structure indicates that the highest peak at  $0.2370974 \text{ s} \pm 0.1 \text{ } \mu\text{s}$  is most likely to be the true period. In addition to these analyses, the period is detected weakly in those individual orbits having more than 1,500 s of exposure. There is no evidence for orbital motion or a secular change in period  $P$  during the span of these observations. On a timescale of two days, the upper limit on  $\dot{P}$  is  $2 \times 10^{-12} \text{ s s}^{-1}$ , and  $\Delta v$  is less than  $0.5 \text{ km s}^{-1}$ . We conclude that the 0.237-s period is not an instrumental artefact, because similar analyses on background counts collected at different positions in the detector do not reveal a signal. We do not detect a significant signal at any other period, including previously reported periods<sup>11-13</sup> near 60 s, even though the PSPC is at risk of manufacturing spurious periods between 30 and 400 s because of the deliberate dithering of the satellite.

Figure 2 shows the folded light curve in three different energy bands, and their sum. The pulse profile has a single broad peak, which is consistent with the absence of power at submultiples of the 0.237-s period. The pulsed fraction is 24% in the band 0.07–0.2 keV and declines with energy. At 0.2–0.28 keV, the pulsed fraction is 19%, and at 0.28–1.50 keV it is 15%. These pulsed fractions are probably lower limits, as there is a known timing error in the processed data which shifts some of the photon arrival times randomly with respect to the phase of the 0.237-s period. The extremely soft spectrum of the pulsations, and the broadness of the pulse profile, are suggestive of thermal emission from the surface of a neutron star. But it is difficult to interpret these data in terms of surface temperature and distance, because the X-ray spectrum in the Rosat bandpass can be modified from the black-body shape as a result of non-grey atmospheric opacity<sup>14</sup>. Strong L and K edges could be present. Rosat has recently detected soft X-ray pulsations from Vela<sup>15</sup>, also in the lowest energy channels.

To study the X-ray spectrum, we extracted all the source counts within a  $2'$  radius, and subtracted background from an annulus between radii of  $2.5'$  and  $4.2'$ . The total flux in the 0.1–2.4-keV band is  $\sim 1.5 \times 10^{-12} \text{ erg cm}^{-2} \text{ s}^{-1}$ , which is roughly

consistent with the Einstein result. The X-ray spectrum is very soft, but it cannot be adequately fitted by a black-body or a power-law spectrum, as illustrated in Fig. 3. We have not yet explored the full range of plausible spectral models, but with the caveat concerning atmospheric opacity in mind, a composite model consisting of a black body of temperature  $T \approx (3-4) \times 10^5 \text{ K}$  plus a power-law component with energy index  $\alpha$  in the range 0.75–1.75 yields an adequate fit to the data. In

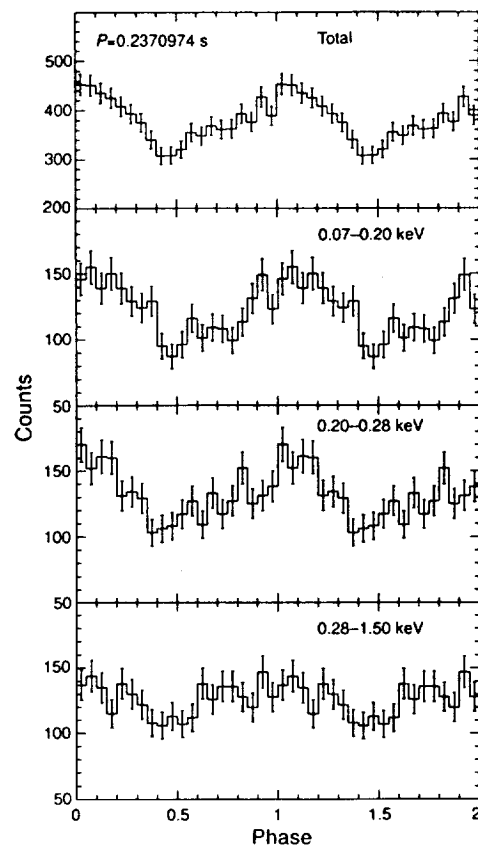
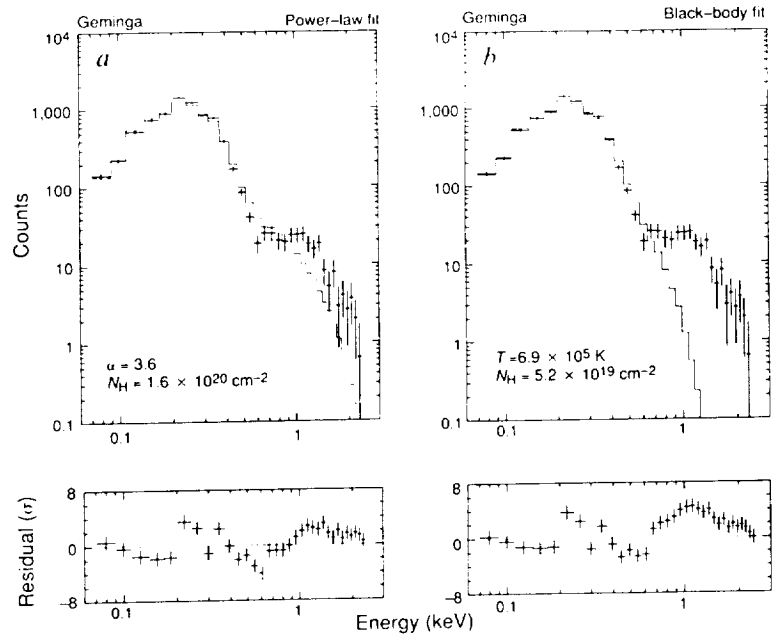


FIG. 2 Pulse profile of all data between 0.07 and 1.5 keV folded into a 20-bin light curve. The top panel is the sum of the bottom three.

FIG. 3 Spectral fits with single-component models. *a*, Power law; *b*, black body.



this model, the decrease of pulsed fraction with energy might be caused by the increasing contribution of an unpulsed synchrotron component. A column density in the range  $(0.5\text{--}3) \times 10^{20} \text{ cm}^{-2}$  is allowed.

Observations indicating that Geminga might be a pulsar somewhat older than Vela have been reviewed previously<sup>3-6,8</sup>. The overall energy distributions of the two objects are similar at wavelengths from optical through  $\gamma$ -rays. The ratio of  $L_\gamma/L_x = 1,000$  is a likely indicator of a pulsar emission mechanism. The ratio  $L_x/L_{\text{opt}} \approx 1,800$ , and the soft X-ray spectrum, also suggest an isolated neutron star. The discovery of a short pulse period fulfils this expectation. A detailed theoretical model for  $\gamma$ -ray pulsars was developed by Ruderman and Cheng<sup>9</sup>, who proposed an evolutionary scheme in which a short-period  $\gamma$ -ray pulsar evolves from a Crab-like stage, through that of Vela, and finally reaches that of Geminga. In the regime of Vela-like pulsars,  $\gamma$ -rays are produced in the outer magnetosphere as synchrotron radiation from electron-positron pairs. As it slows down, such a pulsar uses an ever increasing fraction of its spin-down power in the production of an  $e^\pm$  wind and associated  $\gamma$ -ray emission until almost the full spin-down power,  $\sim 4 \times 10^{36} \text{ erg s}^{-1}$ , goes into this mechanism. As the period increases further, the currents necessary to sustain pair production are quenched and the  $\gamma$ -ray emission ceases. They predicted that Geminga is near the turnoff period, which for Vela itself would be  $\sim 0.13 \text{ s}$ , and postulated that ordinary pulsars avoid this fate because they have more highly curved magnetic field lines near the polar cap, which can maintain the potential drop required for pair production.

The theory was generalized by Chen and Ruderman<sup>16</sup>, who argued that there is actually a death line for Vela-like (outer gap) pulsars given by  $5 \log B - 12 \log P = 72.2$ , where  $B$  is the surface magnetic field. If Geminga is to fall near this line, it must have  $B \approx 1 \times 10^{13} \text{ G}$ , only a factor of 3 greater than that of Vela. In this case, the total spin-down power,  $\dot{E} \approx B^2 R^6 \Omega^4 / c^3$ , would be  $\sim 1.8 \times 10^{36} \text{ erg s}^{-1}$ . As the observed  $\gamma$ -ray flux<sup>1</sup> is at least  $2.4 \times 10^{-9} \text{ erg cm}^{-2} \text{ s}^{-1}$ , an upper limit to the distance is  $2,500 (B/10^{13}) \text{ pc}$  for the luminosity not to exceed the estimated spin-down power. (The column density derived from the X-ray spectrum almost certainly restricts the distance to less than 500 pc.) The predicted magnetic field would result in a spin-down rate of  $4 \times 10^{-13} (B/10^{13})^2 \text{ s s}^{-1}$ , significantly below the upper limit of  $2 \times 10^{-12}$  established by this observation. A second observation could easily determine  $\dot{P}$ , and thus the magnetic field. The fact that Geminga is not detected in high-energy X-rays

or low-energy  $\gamma$ -rays<sup>17</sup> is consistent with the outer gap model. The low-energy cutoff of the spectrum at a frequency  $\omega_c$  is determined by the energy of the  $e^\pm$  pairs that leave the magnetosphere before losing their energy to synchrotron radiation. Because  $\omega_c \propto \Omega^{-2} B^{-3}$ , scaling from the Vela break at  $\sim 1 \text{ MeV}$  (ref. 7) predicts a break at  $\sim 25 \text{ MeV}$  for Geminga. Other pulsars that may be progenitors of the Geminga-like  $\gamma$ -ray pulsars are PSR1509-58 (ref. 18) with  $P = 0.150 \text{ s}$  and PSR1706-44 with  $P = 0.102 \text{ s}$ . These both fall in the region of Vela-like pulsars<sup>16</sup>, and were recently detected<sup>19,20</sup> by the Compton Gamma Ray Observatory (CGRO).

Our results thus largely confirm the expectation that Geminga is a pulsar similar to Vela. The absence of a synchrotron nebula around Geminga remains a fundamental difference, which is perhaps related to the fact that Geminga has the longest period of the  $\gamma$ -ray pulsars. We suggest that many of the other unidentified high-energy  $\gamma$ -ray sources are spinning neutron stars which are 'radio quiet', or whose radio beams do not intersect the Earth. Rosat should be able to identify  $\gamma$ -ray pulsars by finding the periods of sources detected by CGRO in the galactic plane.  $\square$

Received 30 March; accepted 28 April 1992.

1. Fichtel, C. E. *et al. Astrophys. J.* **196**, 163-182 (1975).
2. Swanenburg, B. N. *et al. Astrophys. J.* **243**, L69-L73 (1981).
3. Bignami, G. F., Caraveo, P. A. & Lamb, R. C. *Astrophys. J.* **272**, L9-L13 (1983).
4. Bignami, G. F. *et al. Astrophys. J.* **319**, 358 (1987).
5. Halpern, J. P. & Tytler, D. *Astrophys. J.* **330**, 201-217 (1988).
6. Bignami, G. F., Caraveo, P. A. & Paul, J. A. *Astr. Astrophys.* **202**, L1 (1988).
7. Spoelstra, T. A. & Hermesen, W. *Astr. Astrophys.* **135**, 135-140 (1984).
8. Halpern, J. P. in *Proc. GRO Science Workshop* (ed Johnson, N.) 4-166-4-173 (1989).
9. Ruderman, M. & Cheng, K. S. *Astrophys. J.* **335**, 306-318 (1988).
10. Trümper, J. *et al. Adv. Space Res.* **2**, 241-249 (1983).
11. Bignami, G. F., Caraveo, P. A. & Paul, J. A. *Nature* **310**, 464-469 (1984).
12. Bignami, G. F. in *The Origin and Evolution of Neutron Stars* (eds Helfand, D. J. & Huang, J. H.) 465-474 (Reidel, Dordrecht, 1987).
13. Caraveo, P. A. & Bignami, G. F. in *The Origin and Evolution of Neutron Stars* 545 (eds Helfand, D. J. & Huang, J. H.) (Reidel, Dordrecht, 1987).
14. Romani, R. W. *Astrophys. J.* **313**, 718-726 (1987).
15. Ogelman, H., Finley, J. P., Aschenbach, B., Trümper, J. & Zimmermann, U. *Bull. Am. astr. Soc.* **23**, 1349 (1991).
16. Chen, K. & Ruderman, M. *Astrophys. J.* (in the press).
17. Bignami, G. F. & Hermesen, W. *Astr. Astrophys.* **21**, 67-108 (1983).
18. Seward, F. D. & Harnden, F. R. H. Jr *Astrophys. J.* **256**, L45-L47 (1982).
19. Wilson, R. B., Finger, M. H., Fishman, G. J., Meegan, C. A. & Paciesas, W. S. *IAU Circ. No. 5429* (1992).
20. Kniffen, D. A. *et al. IAU Circ. No. 5485* (1992).

ACKNOWLEDGEMENTS. We thank F. R. Harnden and F. Seward for making the barycentric correction, and for assistance with the data analysis. We thank G. Bignami for his review. This work was supported by NASA through a Rosat guest observer grant.